Potential of hyperspectral imagery for geophysical applications

Rodolphe MARION* & Rémi MICHEL rodolphe.marion@cea.fr

***Chairman, French Hyperspectral Permanent Working Group, 2009**

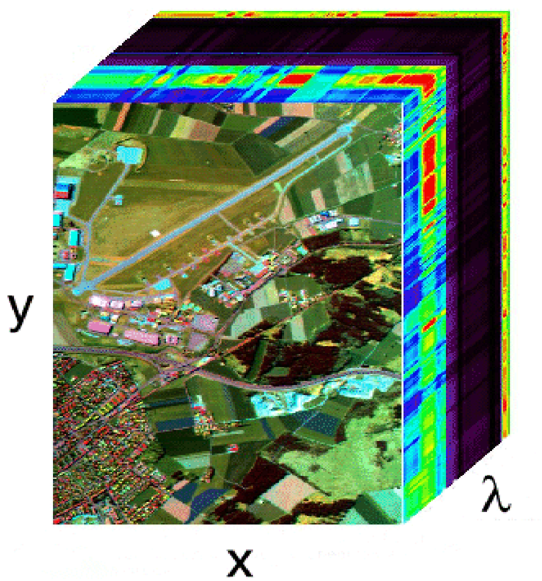

Monitoring Earth Surface Changes
from Space

October 28 – 30, 2009

Principles of hyperspectral data acquisition

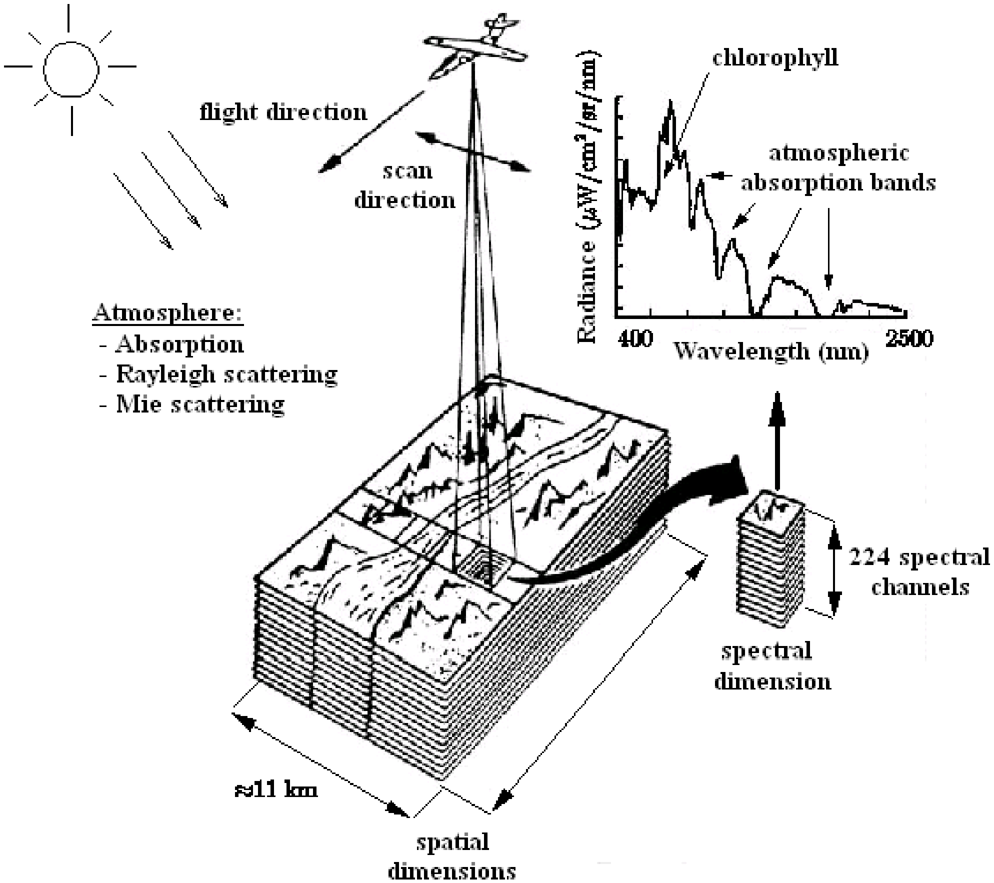

Image acquisition (AVIRIS airborne sensor example)

- Typical characteristics of hyperspectral images:
  - Scene # 10km x 10km
  - Spatial resolution # 10m
  - Spectral coverage # 0.4-2.5μm
  - Number of spectral bands # 200
  - Spectral resolution # 10nm

hyperspectral datacube

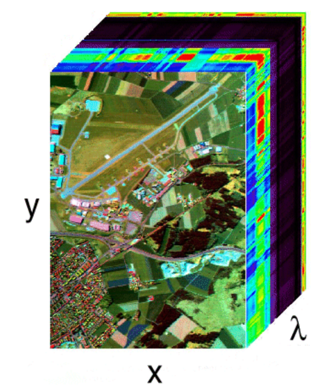

Each pixel of the image is a « continuous » spectrum containing detailed information on ground and atmosphere

Hyperspectral imagery is generally qualified as imaging spectroscopy

Physics of the image

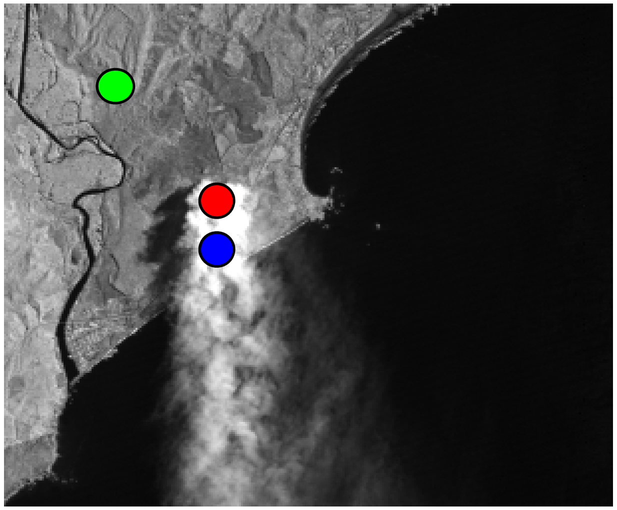

AVIRIS image of Quinault fire

- Vegetation
- Aerosols + thermal
- Aerosols

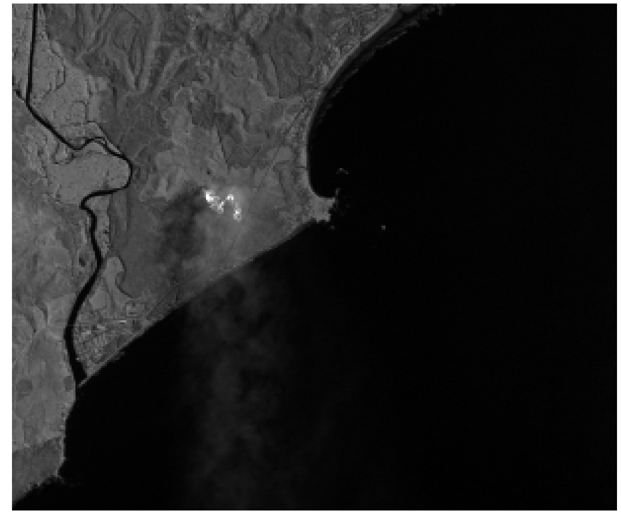

aerosol plume signal

vegetation chlorophyll red-edge

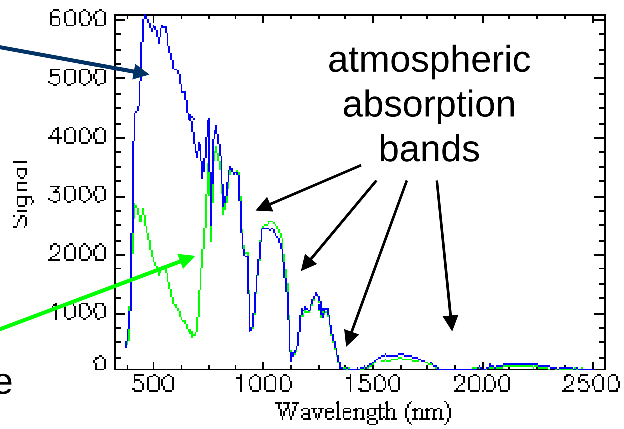

atmospheric absorption bands

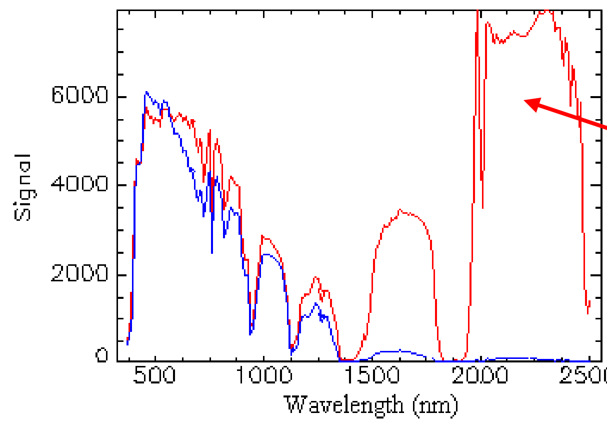

thermal emission of the fire

- **When physics is taken into account, hyperspectral imagery can be used to retrieve <u>quantitative physical information</u> from the scene (ground and atmosphere)**
- **Therefore, it brings information on the <u>nature</u> of objects AND eventually on their <u>status</u> (stressed vegetation, wet soil…)**
- **Hyperspectral imagery is <u>complementary</u> to other modalities (visible, thermal, radar)**

A favorable international context

- Current sensors (mainly airborne):
  - **AVIRIS ([0.4-2.5µm], 224 bands, NASA)**
  - **CASI ([0.4-0.95µm], 20 bands, Itres)**
  - **HYDICE ([0.4-2.5µm], 210 bands, NRL)**
  - **DAIS ([0.4-12.5µm], 211 bands, DLR)**
  - **HyMap ([0.4-2.5µm], 126 bands, HyVista)**
  - **MIVIS ([0.4-12.5µm], 102 bands, Sensytech)**
  - **APEX ([0.4-2.5µm], 300 bands, ESA)**
  - **Hyperion ([0.4-2.5µm], 196 bands, NASA)**
    - The only sensor on-board satellite !!!

CASI airborne sensor

- Satellite projects:
  - **Artemis (USA) : launched May 2009 (US military applications only)**
  - **EnMap ([0.4-2.5µm], 270 bands, 30m, DLR) : 2012-2013**
  - **PRISMA ([0.4-2.5µm], 200 bands, 20m + PAN 5m, ASI) : 2012-2013**
  - **Others: Hyper-X (Japan), HERO (Canada), MSMI (South Africa) ???**
  - **France : CNES working group, phase 0…**

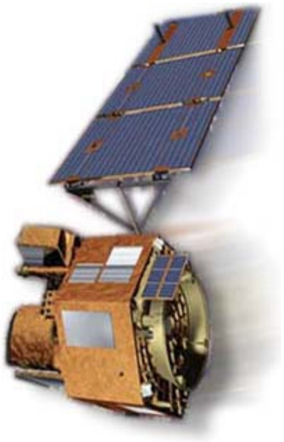

Hyperion sensor on-board EO-1 satellite

Increased availability of hyperspectral data in a near future…

Overview of scientific applications

- **Atmospheric parameters (gas, aerosols…) useful for:**
  - Surface phenomenon detection (fires, volcanoes, methane emissions…)
  - Pollution estimation in the boundary layer
- **Geosciences:**
  - Geology, mineralogy, mining and oil prospecting, soils quality, degradation and pollution, volcanism, crisis management…
- **Vegetation:**
  - Biochemical content (pigments, water, dry matter…)
  - Canopy structure (Leaf Area Index…)
  - Fluorescence, stress detection…
- **Urban and natural hazards:**
  - Hyperspectral data usefulness is limited because of its low spatial resolution. A interesting perspective: fusion
- **Coastal waters:**
  - Water quality, benthic communities, bathymetry, bottom types, see-ground interface…

Quinault biomass burning aerosol plume analysis by hyperspectral imagery*

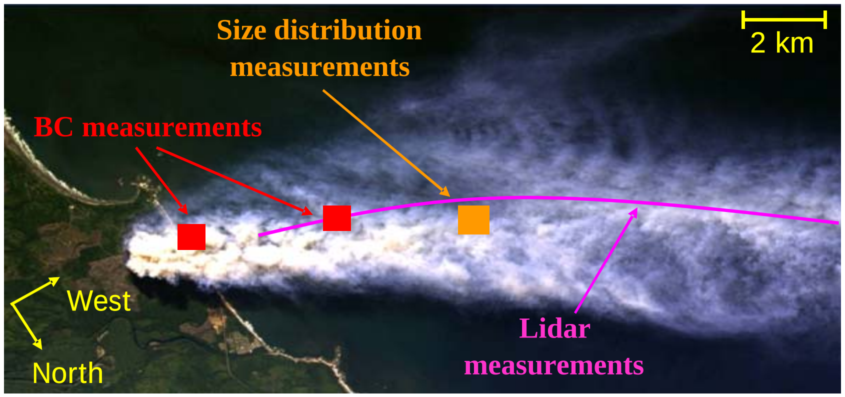

BC : Black Carbon

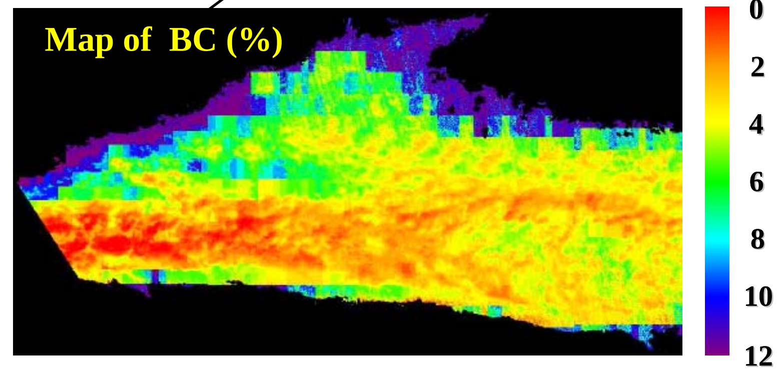

AVIRIS image of Quinault Fire (USA)

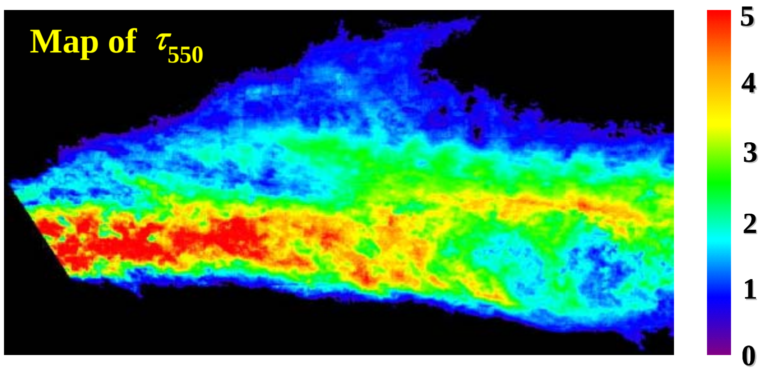

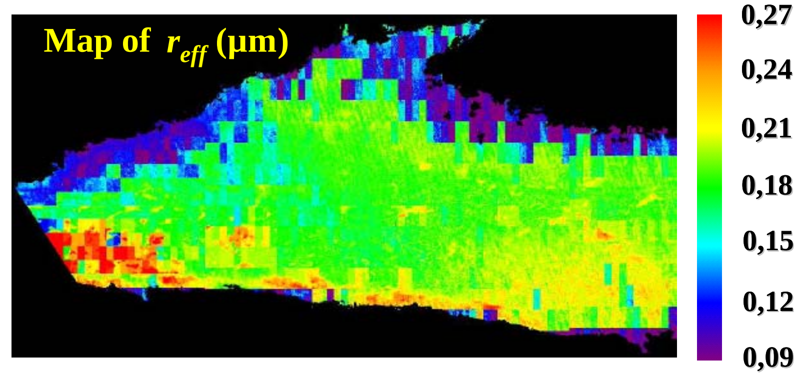

In situ measured parameters (samples , lidar) and estimation from the image (concentration τ_{550}, composition BC, size distribution r_{eff}) are in adequacy

* A. Alakian, R. Marion, and X. Briottet, “Remote sensing of aerosol plumes: a semianalytical model,” *Applied Optics*, Vol. 47, No. 11, pp. 1851-1866, 10 April 2008
* A. Alakian, R. Marion, and X. Briottet, “Retrieval of microphysical and optical properties in aerosol plumes with hyperspectral imagery: L-APOM method,” *Remote Sensing of the Environment*, Vol. 113, No. 4, pp. 781-793, 15 April 2009

Carbon dioxide of Pu`u`O`o volcanic plume at Kilauea retrieved by AVIRIS hyperspectral data*

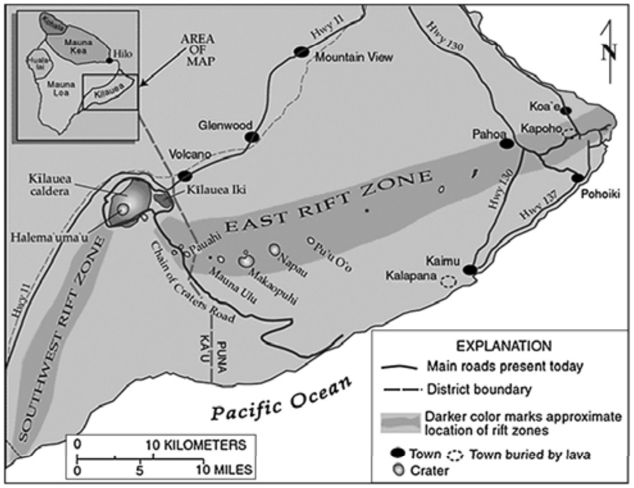

Location map of Kilauea on Big Island, Hawaii, USA (Johnson, 2000)

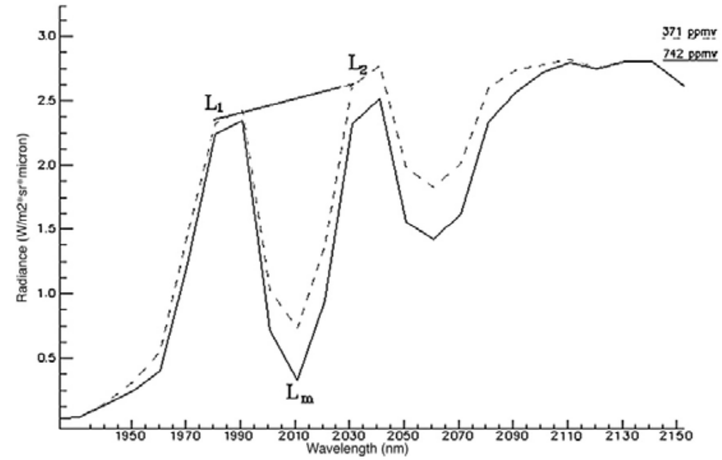

CO_2 absorption bands near 2 µm used by the CIBR technique

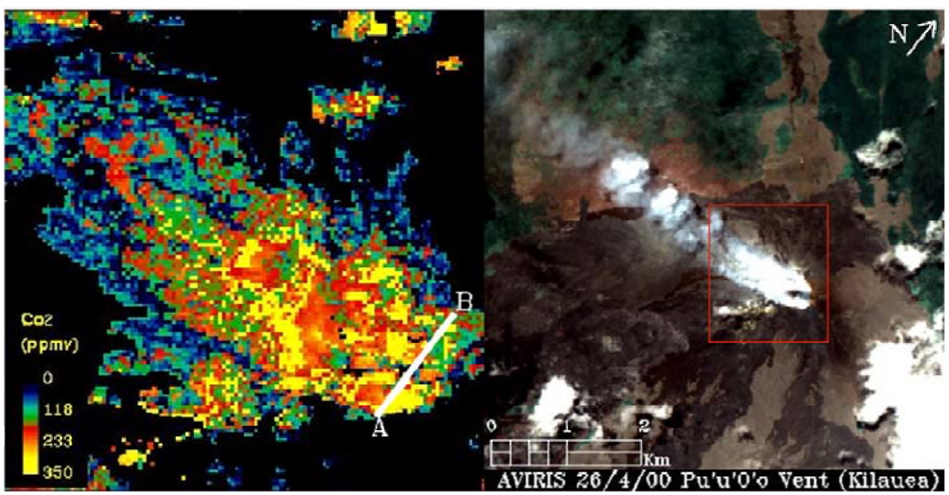

Map of volcanic plume carbon dioxide (left) and AVIRIS image of Pu`u `O`o Vent plume (right)

* C. Spinetti, V. Carrère, M. F. Buongiorno, A. J. Sutton, T. Elias, “Carbon dioxide of Pu`u`O`o volcanic plume at Kilauea retrieved by AVIRIS hyperspectral data,” *Remote Sensing of the Environment*, Vol. 112, pp. 3192-3199, 2008

Geology (mineral mapping at Cuprite) [1/3]

AVIRIS image (λ_R=2.1µm, λ_G=2.2µm, λ_B=2.34µm)

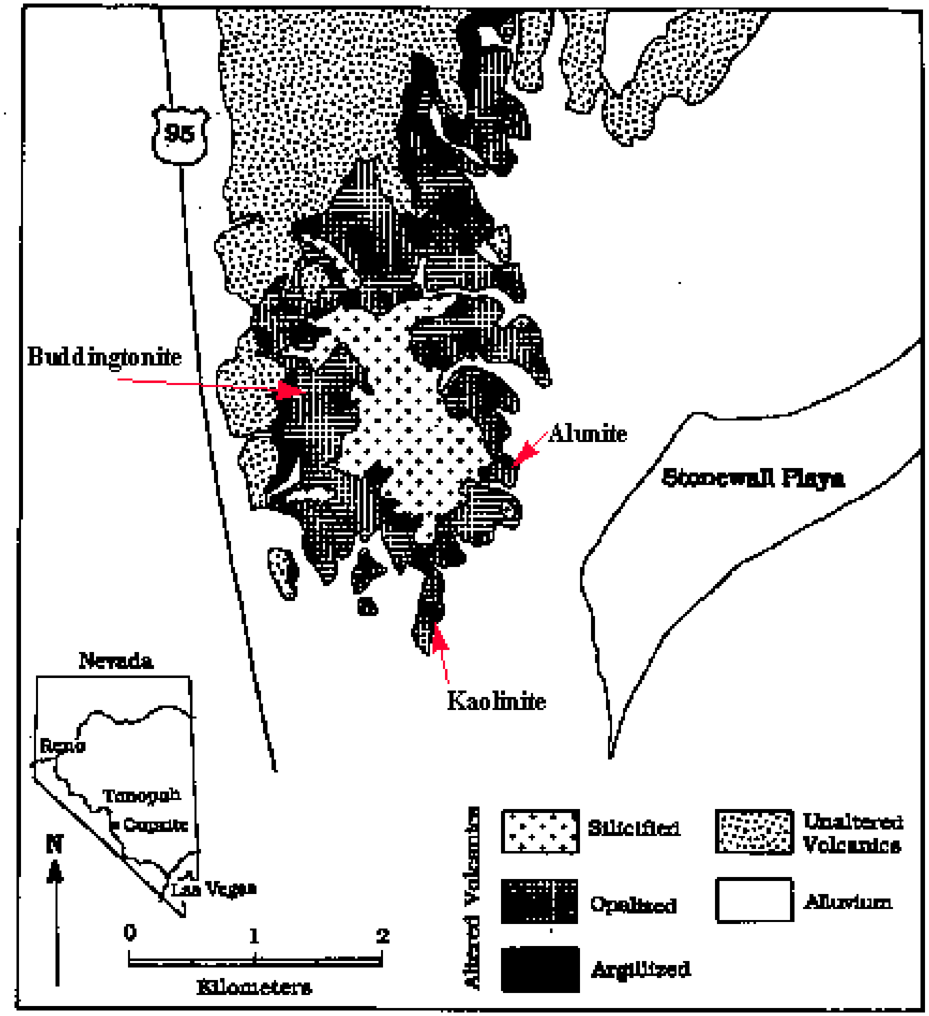

Geological map of the site

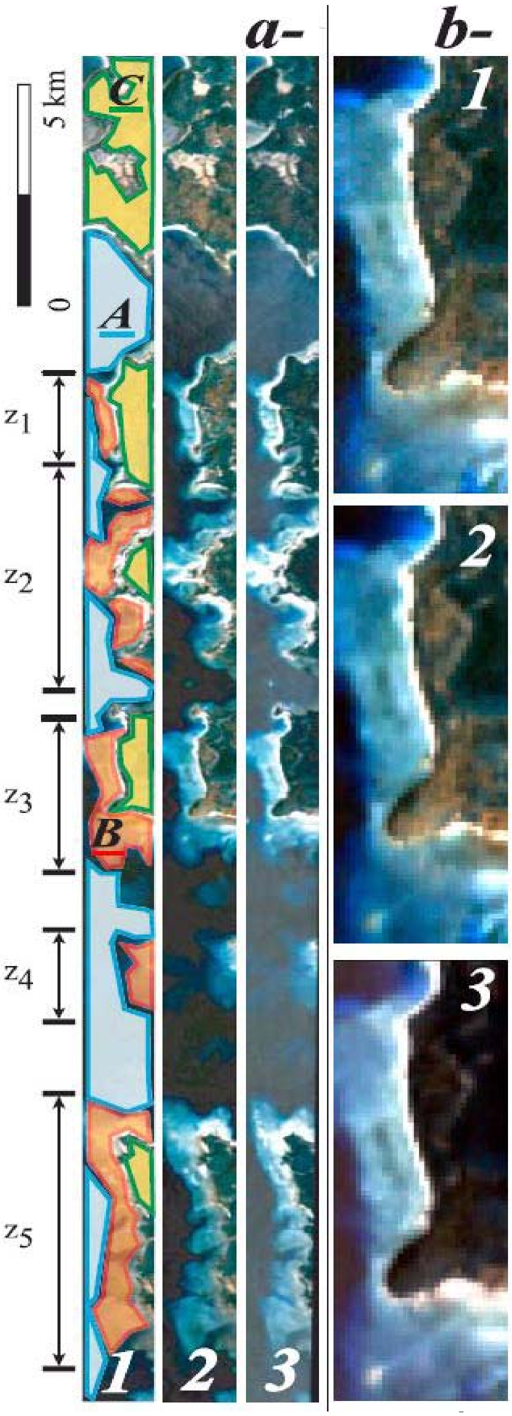

Technique

Table 1. Hyperion Hyperspectral Images and Sea Level Used in the Present Study[a]

		Image Reference	Date	Site Longitude	Site Latitude	Sea Level (m)
1	PRE	EO1134051200404911OPY	18 February 2004	92.8842	13.3422	1.42
2	PRE	EO1134051200406511OPY	5 March 2004	92.8842	13.3422	1.64
3	POST	EO1134051200504211OKZ	11 February 2005	92.8000	12.5000	1.90

[a]Images acquired to minimize effects of seasonal variations on radiative transfer. Theoretical sea level from tide gauge at Port Blair, South Andaman Islands (http://www.shom.fr/).

$$R = R_g + R_w + (R_b - R_w)e^{-2Kz}$$

R= surface reflectance
Rg =sea surface contribution
Rw = deep water subsurface scattering contribution of photons that did not reach the sea bottom
z = depth of the water column
K =effective attenuation coefficient (upwelling and downwelling)

$$K = \frac{1}{2(z_1 - z_2)} \log\left[\frac{R_2 - (R_g + R_w)_2}{R_1 - (R_g + R_w)_1}\right] = \frac{1}{2(t_1 - t_2)} \log\left[\frac{R_2 - (R_g + R_w)_2}{R_1 - (R_g + R_w)_1}\right].$$

$$U = t_3 - t_1 + \frac{1}{2K} \log\left[\frac{R_3 - (R_g + R_w)_3}{R_1 - (R_g + R_w)_1}\right].$$

U= tectonic uplift estimated for each wavelength and then averaged over the spectral range (570–690 nm)

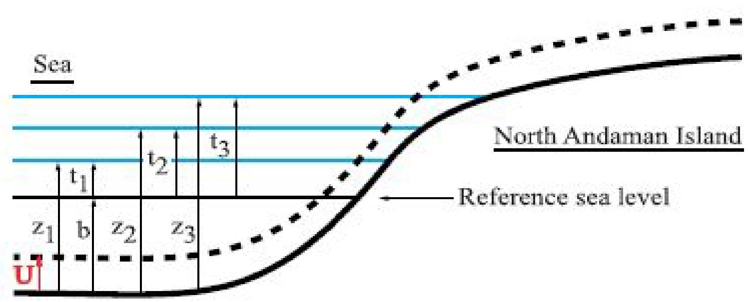

Comparison with other techniques

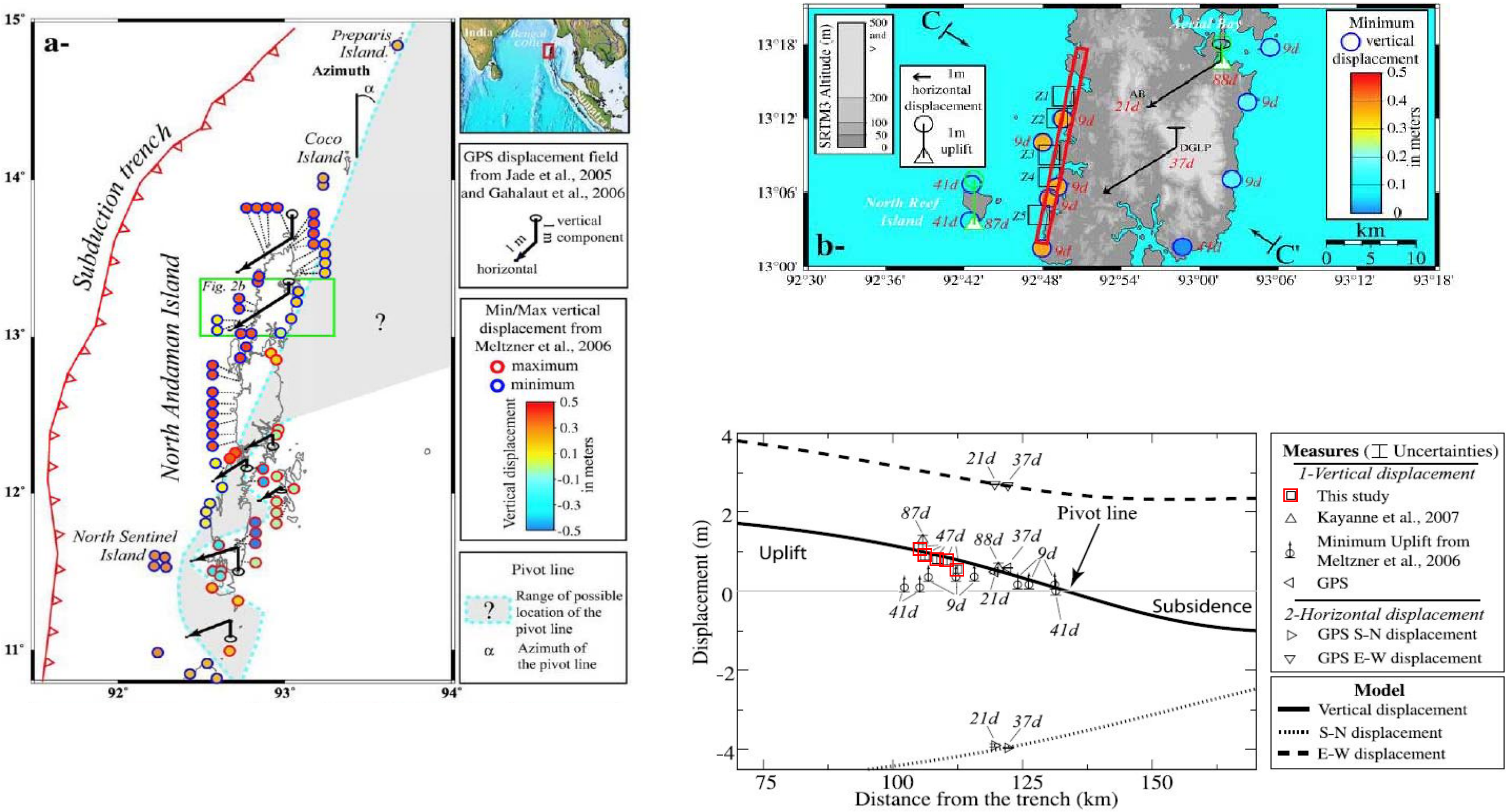

Smet, S., R. Michel, and L. Bollinger (2008), “Uplift of the 2004 Sumatra-Andaman earthquake measured from differential hyperspectral imagery of coastal waters,” *J. Geophys. Res.*, 113, B09403, doi:10.1029/2007JB005317